Available online at http://bjas.bajas.edu.iq
https://doi.org/10.37077/25200860.2021.34.2.04
College of Agriculture, University of Basrah

Basrah Journal of Agricultural Sciences

ISSN 1814 – 5868 Basrah J. Agric. Sci. 34(2) 42-59, 2021 E-ISSN: 2520-0860

Antitumor Activities of Biosynthesized Silver Nanoparticles using *Dodonaea viscosa* (L.) Leaves Extract

Zainab F. H. Al-Musawi[1] & Narjis H. M. Al-Saadi[2*]

[1,2] Department of Chemistry, College of Science, University of Kerbala, Kerbala, Iraq

[2*]**Corresponding author email:** narjis.h@uokerbala.edu.iq; zainab.fasal@uokerbala.edu.iq

Received 28th January 2020; Accepted 13th April 2021; Available online 1 November 2021

Abstract: Biosynthesis of silver nanoparticles (AgNPs) from plant extracts is considered one of the green chemistry methods, as this method is characterized by ease, fast and low cost to manipulate. Interestingly, AgNPs have an important role, especially in nano-medicine. Using AgNPs for cancer therapy are an affordable way to control tumor growth and constitute a choice strategy to fight cancer cells. First type of conventional cancer treatment is surgical treatment then radiation and chemotherapy. However, these treatments may work for some cancer subtypes, and have various side effects, in most cases, with high doses. In this study, silver nanoparticles **(**AgNPs) were biosynthesized using *Dodonaea viscosa* leaves extract. The formation of these particles was confirmed through the color change, UV-Visible Spectrophotometer displaying at 463nm.While the particles characterization was done by Surface Plasmon Resonance (SPR) band and Fourier Transform Infra-Red (FT-IR) spectroscopy which revealed the effective functional groups that have ability to bio-reduction silver ion Ag^{+}. In addition, X-ray diffraction (XRD) determined the crystal structure of silver nanoparticles, as shown by the peaks at 2θ values of 38.1874, 46.2491, 57.5409 and76. 8313°.The atomic force microscopy (AFM) analysis showed the size and the surface properties of biosynthesized nanoparticles, and the silver nanoparticles had an average size of 60.22 nm. Finally, scanning electron microscopy (SEM) showed spherical shape of AgNPs and having different average diameter D1 (21.10), D2 (21.39) and D3 (11.86) nm. *In vitro*, the synthesized AgNPs exhibited potential anti-tumor activities against human lung cancer (A549) and ovarian cancer (SK-OV-3) carcinoma cell lines in a dose-dependent manner with IC_{50} of 1.73 and 2.23µg.ml^{-1}, respectively. Our results showed the promising use of AgNPs as an alternative treatment for cancer cells directly and selectively on A549 cell line at concentrations (2.000, 1.699, 1.398 and 1.301 µg /mL).

Keywords: Silver nanoparticles, *Dodonaea viscosa*, Anti-tumors, Biosynthesis

Introduction

Nanotechnology is one of the techniques through which nanoparticles can be synthesized. This field has many applications in various life requirements likes (biomedical sciences, energy science, mechanics, optics, and magnetics). Besides, nano-biotechnology uses the biological system to synthesize nanoparticles (NPs), which revolutionized agricultural science and modern medicine; Gopinath *et al*., 2016; (Yadi *et al*., 2018)..

Nanotechnology specializes in studying small objects with a scale of (1-100) nanometers (Abdelghany *et al*., 2018). Metallic nanoparticles synthesis involves physical, chemical, or biological processes (Bedlovičová & Salayová, 2017). Yet, most of these methods are unfriendly to the environment and require high energy and heat (Netala *et al*., 2016). A cleaner and safer alternative procedure is green synthesis of nanoparticles. The nanoparticles synthesis method follows a biological process based on using the plant and micro-organism′s extract like (bacteria, yeast, fungi, and algae) as a medium for the synthesis process *(*Singh *et al.,* 2017). Plant extracts contain natural reducing agents such as phenols and other reducing agents that can reduce some metals and convert them into nanoparticles (Otunola & Afolayan, 2018). Likewise, the natural enzymes, proteins, flavonoids, and antioxidant chemical compounds found in microorganisms and plants are used to reduce and stabilize metals during the synthesis of NPs. Gold, silver, copper, titanium, iron, platinum, and lead are metals used for synthesizing nanoparticles. Silver nanoparticles are the most commonly used because they have wide range of biomedical and industry applications (Revathi & Dhanaraj, 2019)..

Dodonaea viscosa is a type of plant that contains alkaloids, flavonoids, fixed oil and fat, steroids, phenolics, saponins, tannins, gums, mucilage, carbohydrates, reducing sugar, glycosides, and trace elements. (Al-Snafi, 2017). Different parts of the *Dodonaea viscosa* plant are used in various therapeutic applications; for example, stems and leaves are used to treat fever, where seeds (coated in honey in conjunction with other plants) are used to treat malaria, the leaves also are used relieve swelling aches and itching, fevers and as an antispasmodic agent (Hamadi, 2017; Mahyoub, 2019; Alasmari, 2020). Nanotechnology has been used to synthesis nanoparticles using some plant extracts as biochemical agents to convert metal ions into NPs. This study aims to synthesize AgNPs from the *D. viscosa* extract and test its potential therapeutic effect as an anti-tumor treatment.

Materials & Methods

Collection of Plant

Fresh *D. viscosa* leaves were collected from the garden of the University of Kerbala College of Science from 1 September to 30 October. First, the leaves were washed using tap water and then deionized water, then they are left to dry room at temperature. Finally, the dry leaves were cut into small slices and stored in a dark and dry place for further use to prepared extract. The identification of the plant species was done by the botanist Dr. Nibal Muteer at the University of Kerbala, College of Education of Pure Science.

Materials

The chemical reagents used in this study were purchased from Hi-Media Laboratories (India), Reagent World Inc. (USA), Merk (USA), and MTT Kit Intron Biotech (Korea).

Preparation of Aqueous *D. viscosa* Extract

Ten grams of small pieces of dry leaves were added into deionized water (200 mL) and boiled for 10 minutes (Balashanmugam and Kalaichelvan, 2014). Followed, the crude extract was filtered by using filter paper Whatman No.1 (42µm). The same filtrate

extract was used to synthesize the silver nanoparticles (AgNPs).

Qualitative phytochemical analysis of *D. viscosa* leaf extract

Gas chromatography and mass spectroscopy, GC-MS, is a type of analysis that incorporates the characteristics of gas-chromatography and mass spectrometry to find various materials inside the sample. GC-MS was used to analyze the chemical constituents of *D. viscosa* leaf extract. This analysis was done at the University of Kashan, Iran. In brief, the instruments use electron ionization with two columns, while Helium, Nitrogen, and Zero air was used as carrier gas. The oven temperature was 400°C, and the chromatogram of GC-MS for organic compound was detected by contrasting their spectra with standard values contained in the computer library (Flaih & Al-Saadi, 2020).

Synthesis of Silver Nanoparticles (AgNPs)

An aqueous solution (1 mM) of silver nitrate was prepared to use in (AgNPs) synthesis and aqueous extract (3, 5, and 7 mL) respectively were added to 45 mL of $AgNO_3$ and the best volume was 3 mL. The mixture was shaken and then incubated for 24 hours at 45 °C. The pellets of formed nanoparticles were collected by centrifugation at 5300 xg for 15 minutes (Revathi & Dhanaraj, 2019). Then the obtained pellets were washed three times with distilled water before they were dried and stored in a dark, dry place at room temperature for further use.

Effect of boiling time and extract volume of plant extract on AgNPs synthesis

The influence of boiling time of the plant leaves in preparation the aqueous extract of *D.viscosa* was considered in this study. Ten grams of dry leaves were boiled for (10, 15, and 20 min) with 200 mL of deionized water. Using the UV-Vis Spectrophotometer, the color change in the solution from yellow to brown was detected at different time periods.

To study the effect of extract volumes on particles synthesis, different volumes of plant extract (3, 5, and 7 ml) respectively were added to 45 mL of $AgNO_3$ (1mM) solution. Synthesized silver nanoparticles were observed using a spectrophotometer and the change of color was followed with time (Birla *et al.*, 2013; Moosa *et al.*, 2015).

Characterization of Silver Nanoparticles

UV-Visible Spectroscopy

The silver NPs were tracked by a color change and UV-Visible absorption spectra. The absorbance of the solution mixture was measured at different periods, and the maximum absorptions were scanned by using Ultraviolet-visible spectroscopy (UV-1800/ Kyoto, Japan) at the range from 300 to 700 nm. (Flaih and Al-Saadi, 2020).

Fourier-Transform Infrared Spectroscopy

FT-IR analysis was used to compare the IR spectra before and after formation of AgNPs via *D. viscosa* leaves extract. FT-IR spectroscopy is commonly used to examine interactions between NPs and capping agents. Using this method, the interactions of the functional groups and the metal NPs can be checked when there is more than one functional group in the capping agent. AgNPs were measured with the KBr disk in the wavenumber range between 400 to 4000 cm^{-1} using

Shimadzu (8400S)/Japan FT-IR spectrophotometer (Gomaa, 2017).

X-ray Diffraction

The average grain size, crystallinity, strain, and crystal defect were characterized using XRD (Philips Xpert /Holland XRD). Cu-kα radiation (k=1.50456) was used in the range of (10^o to 80^o). Using Scherer's equation, the crystal size of all prepared samples was calculated as follows:

$$D=\frac{0.9\lambda}{\beta\cos}$$

Where D is the average size of crystallite, lambda (λ) is the X-ray wavelength, θ is the angle of Bragg in radians, and β is the full width in radians at half the maximum of the peak.

Atomic Force Microscopy (AFM)

Using atomic force microscopy, (CSPM Scanning Probe Microscope / Switzerland), the nanometer scale and surface properties of biosynthesized nanoparticles were visualized. The highest measurement was obtained using AFM image analysis software.

Scanning Electron Microscopy (SEM)

A scanning electron microscope (SEM) is a kind of electron microscope that scans the surface to create images of a sample with a directed electron beam. The electrons overlap with atoms to reveal information about the surface topography and the sample composition. The sample was examined using Tescan Mira3 SEM /French.

Antitumor Assay

To measure the activity of the AgNPs as anti-tumor agent, *in vitro* study was evaluated against both lung cancer cell line adenocarcinoma human cells (A549), which were obtained from human alveolar cell carcinoma and ovarian cancer cell line (SK-OV-3), which were obtained from Homo sapiens, human, ovary: ascites and compared with normal cells WRL68. The cell viability was determined using tetrazolium dye(3-(4,5-Dimethyl-2-thia-zolyl)-2,5-diphenyl-2H-tetrazolium bromide) (MTT assay), which is a colorimetric assay for measuring cell metabolic activity and depend on the reduction of the tetrazolium salt by actively growing cells actively to form formazan, which is a purple water-insoluble product (Gasque *et al*., 2014). Tumor cells ($1x10^4$cells per well)) have been grown in 96 micro-liter plates flat well, with a final volume of 200 µL. The type of medium fresh complete Roswell Park Memorial Institute – 1640 Medium (RPMI) from 15 to 20 mL was added then by pipetting was used to disperse cells from the wedding surface into growth medium. Using sterilized parafilm to seal the microplate and it is gently held. Plates flat well were incubated for 24 hours at 37°C in 5% CO_2. Following incubation for 24 hours, the medium was extracted, and serial dilutions of the appropriate compounds AgNPs and extract of *D. viscosa* (15, 20, 25, 50, 100 µg. Ml $^{-1}$) were prepared in mixture (ethanol-deionized water) (1:1 v/v), and then applied to the wells. For each concentration, triplicates and positive controls (cells treated with the serum-free medium and water) and negative control (cells treated with the serum free medium) were used. The plates were incubated at 37 °C in 5% CO_2 for a selected exposure time of 24 hours. Followed by adding, 10 µL of MTT solution to each well. Plates were further incubated, 5% CO_2, for 3-4 hrs. at 37°C. A 100 µL of

Dimethyl sulfoxide (DMSO) as a solubilization solution was applied for 30 minutes to each well to remove the medium and produce purple color which indicates cell viability. The absorbance of each well was calculated using an enzyme-linked immune sorbent assay (ELISA) reader (Bio-Rad, Germany) at a wavelength of 575 nm.

$$\text{Viability } \% = \frac{\text{OD sample}}{\text{OD control}} \times 100$$

The experiment was conducted in triplicate and (IC_{50}) value of AgNPs and plant extract, which expresses half of the inhibitory concentration against lung cancer (A549) or ovarian cancer (SK-OV-3) that kill 50% of the cell population. This value was measured from a dose response-inhibition curve (log concentration vs. absorbance) for each of the extract and AgNPs utilizing non-linear regression with graph pad prism statistical program (Version 8).

Statistical analysis

All data obtained from the MTT method were expressed as the mean± standard deviation of three independent experiments. The P-value at ≤ 0.05 considered statistically significant. Statistical significance was implemented utilizing Graph Pad Prism version 8 (Graph Pad Software Inc., La Jolla, CA).

Results

GC-MS analysis

In this study GC-MS was utilized to identify the different biological components of *D. viscosa* leaves extract, where the analysis of the elements revealed the constituents of phytochemical components. The chromatogram of the analysis showed six peaks of most constituents (Fig. 1).

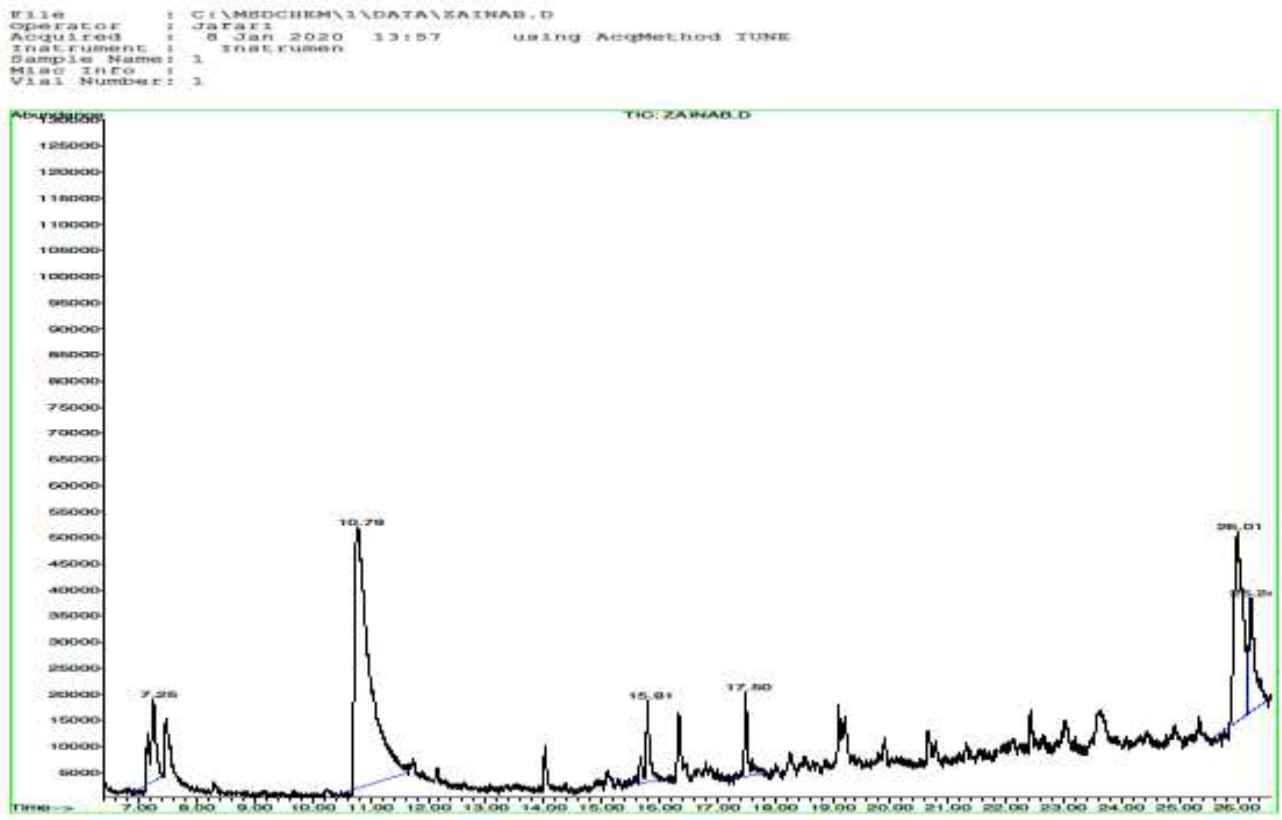

Fig. (1): GC-MS of *D. viscosa* leaves extract.

Table (1): GC-mass analysis of *D. viscosa* leaf extract.

Peak	R. Time	Area %	Name
1	7.25	6.20	Trans -.beta.-Ocimene (+)-4-Carene 1, 3, 6-Octatriene, 3, 7-dimethyl
2	10.79	53.01	Estragole Anethole Estragole
3	15.80	5.35	Pentadecane Pentadecane Pentadecane
4	17.50	4.16	Hexadecane Hexadecane Hexadecane
5	26.01	12.34	9, 12-Octadecadienoic 9, 12-Octadecadienoic 9, 12-Octadecadienoic
6	26.25	9.95	Octadecanoic acid

.

Most of these included 1, 3, 6-octatriene, Estragol, pentadecane, hexadecane, 9, 12-octadecadienoic acid, and octadecanoic acid (Table 1).

The heights of different peaks show the relative concentration of the compounds present in the aqueous extract of *D. viscosa* leaves.

Synthesis of Ag nanoparticles

Aqueous leaves extract of *D. viscosa* was used to synthesize silver nanoparticles (AgNPs). Ag^+ ions were reduced to AgNPs. The crude extract of *D. viscosa* is considered a reducing agent for Ag^+ and chemical stabilizer for AgNPs. The first indication for AgNPs construction was the color change from light yellow to dark brown within 24 hours (Fig. 2). The colorimetric change was detected using a UV-visible spectrophotometer.

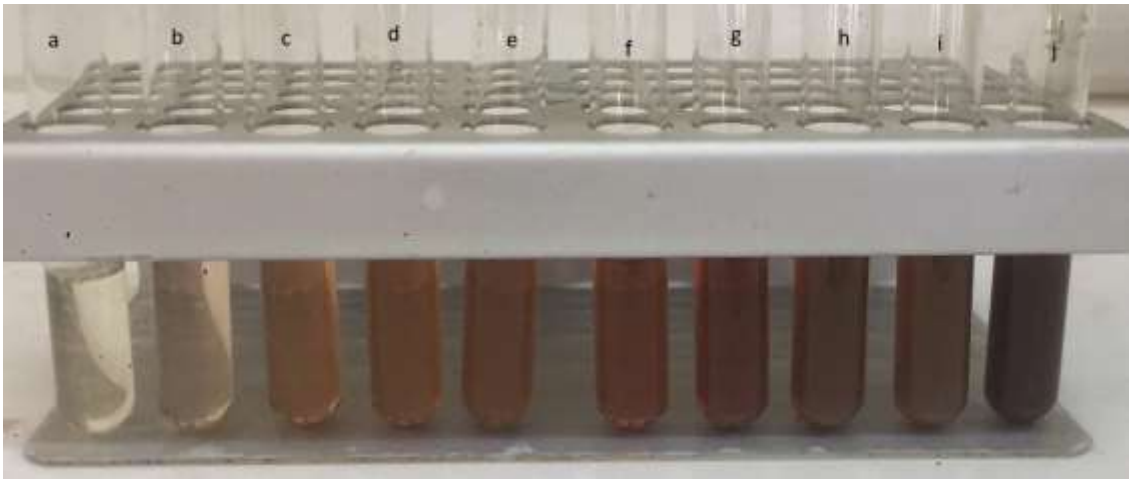

Fig. (2): Biosynthesis of silver nanoparticles (AgNPs) showing the color change with the time. (a) at zero time (b) after 10 min. (c) after 30 min. (d) after 2 hours (e) after 4 hours (f) after 6 hours (g) after 8 hours (h) after 10 hours (i) after 12 hour (j) after 24 hours

UV-Vis Spectroscopy Analysis

Peaks in the absorption spectra represents the produced silver NPs at 463 nm after 24 hours' incubation at 45^{o}C, as shown in (Fig. 3a). The optimal formation of AgNPs was obtained using 3 mL of the leaves extract (Fig. 3b) and a boiling time of 10 min (Fig. 3c). The color change was confirmed using the UV-Vis spectrum.

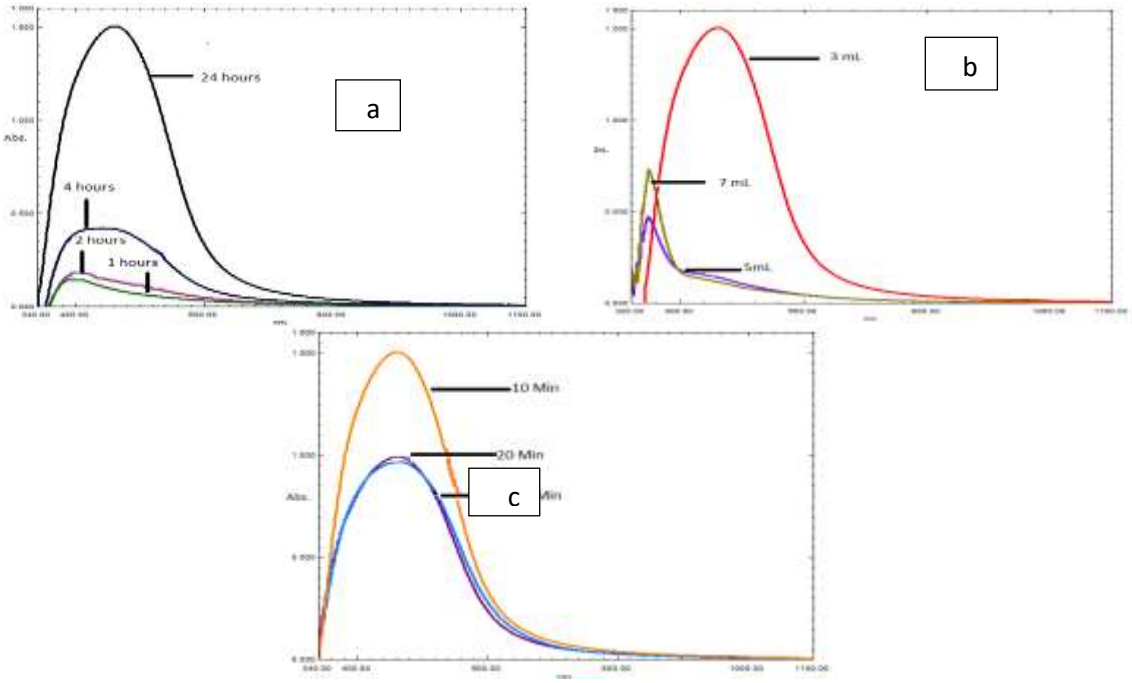

Fig. (3): UV-Visible spectra (a) for silver NPs (b) at different volumes of extract (c) at different boiling time.

Fourier Transforms Infrared Spectroscopy (FT-IR)

Identifying the functional groups for both leaves extract (Fig. 4a) and the synthesized AgNPs (Figure 4b) were carried out using the FT-IR spectrum. The FT-IR spectrum of *D. viscosa* leaves extract showed peaks at 3394.84, 2929.97, 1610.61, 1514.17, 1400.37, 1271.13, 1062.81, 868.00, 650.03 and 542.02 cm^{-1}; while synthesized AgNPs synthesized from *D. viscosa* had spectrum peaks at 3448.84, 2929.97, 1620.26, 1518.03, 1388.79, 1057.03, 873.78 and 692.47 cm^{-1}. The synthesized AgNPs had shifted the absorption peaks from 3394.84 cm^{-1} to 3448.84 cm^{-1} indicating the existence of O-H vibration of phenol, alcohol, and phenol with stretching linkage of N-H of primary, secondary, amides, and amine. In addition, a peak of 2929.97 cm^{-1} was observed, which represents the stretching vibrations of methyl groups (C-H).

Other peaks such as 1610.61and 1514.17 cm^{-1} represent the existence of (C=O) and(C=C), respectively. Moreover, the peaksof1400.37and 1271.13 cm^{-1} were shifted to 1388.79 and 1057.03 cm^{-1}, respectively.

In addition, the band at 650.03cm^{-1} in the leaves extract shifted to 692.47 cm^{-1} in chart of AgNPs. As observed in both leave extract, and the synthesized AgNPs a distinct shift of functional groups' peaks. The distinct bands may reveal some organic compounds like protein, phenolic, or glycosides in plant extract that can act as a reducer and stabilizer to the Ag^{+} ion.

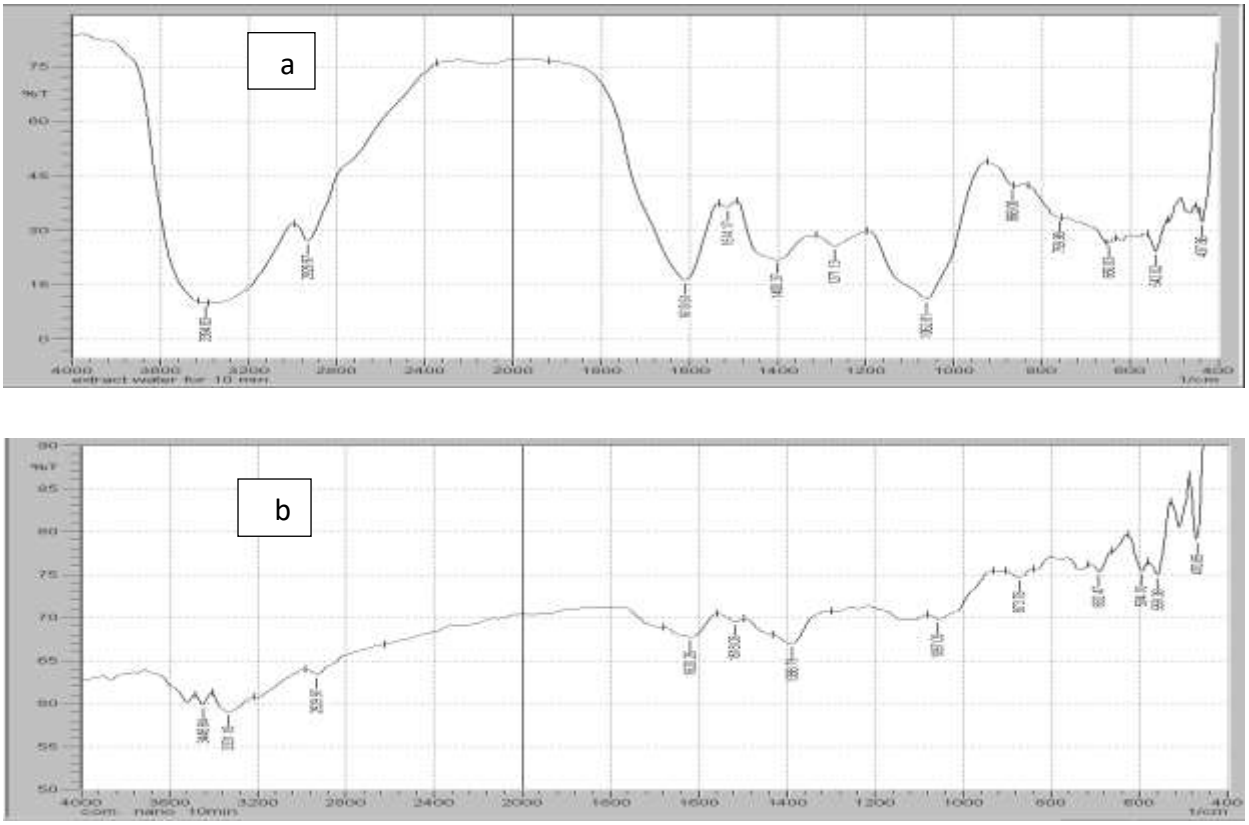

Fig. (4): (a) (FT-IR spectrum of *Dodonea* leaf extract) and (b) (FT-IR spectrum of silver NPs).

(XRD) X-ray diffraction

The crystalline nature of the AgNPs and the single crystals' lattice parameters were verified using X-ray diffraction analysis. The X-ray diffraction analysis revealed five featured peaks at 2θ values of 38.1874º, 46.2491º, 54.8851º, 57.5409º, and 76.8313º (Fig. 5). The average crystal size of AgNPs was estimated to be 37.665 nm. The intensity of 100% was observed at 2θ with 46.2491º. The crystallographic planes of each angle value were also demonstrated and compared with the standard data file of AgNPs.

Atomic Force Microscopy (AFM)

The AgNPs surface morphology (the topography of the surface and the particles' size) was determined using the AFM. AFM holds many advantages in measuring dispersion and particles, as this test would not be affected by the surface oxidation and conductivity. AFM can also measure as small particle size as a sub-nanometer in aqueous fluids (Zhang *et al*., 2016). The measured AgNPs in this study had an average size of 60.22 nm. The two-dimensional and three-dimensional images of the particles, revealed homogenous uniform size and shape, as shown in fig. (6 a, b).

Scanning Electron Microscope (SEM)

AgNPs high magnification images were obtained using SEM technique. This technique can determine morphological features (number, dimension, and shape) of small particles by scanning reflections of a focused beam of electrons over the particles' surfaces. SEM

images of the particles showed spherical shape particles with smooth surfaces morphology, and well scattered with a nearly compact arrangement, as it shown in fig. (7).

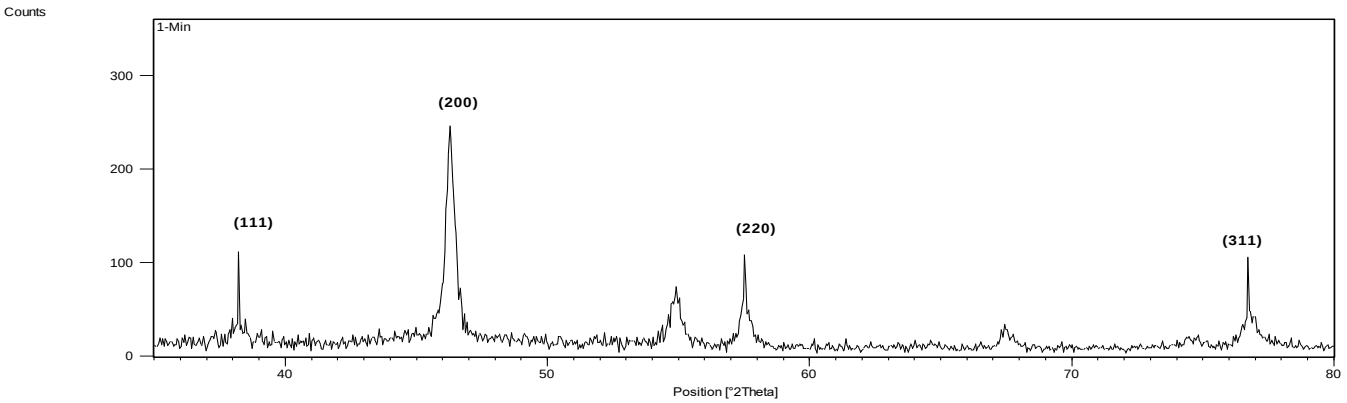

Fig. (5): X-ray diffraction (XRD) of synthesized AgNPs from *D. viscosa* leaf. extract.

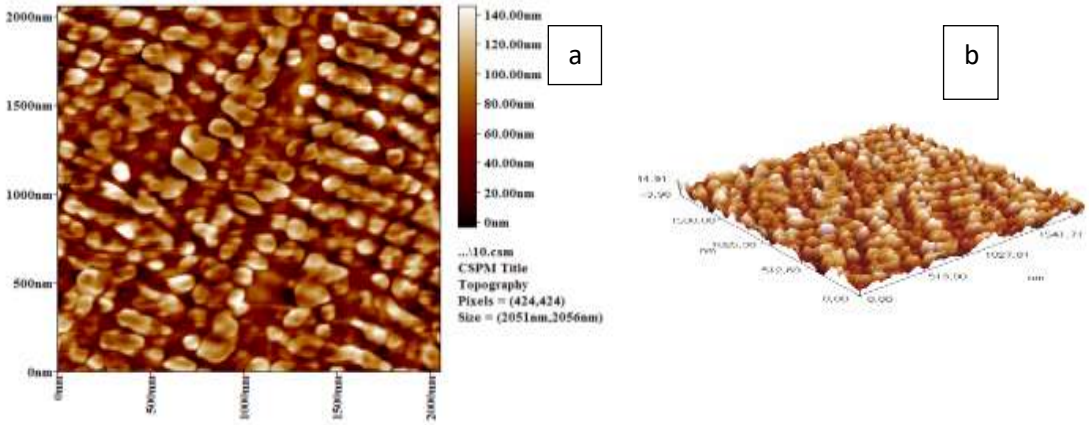

Fig. (6): AFM assay of AgNPs, synthesized by 3 ml of *D. viscosa* aqueous leaf extract for 10 min. (a) Two (2) dimensional image (b) three (3) dimensional image.

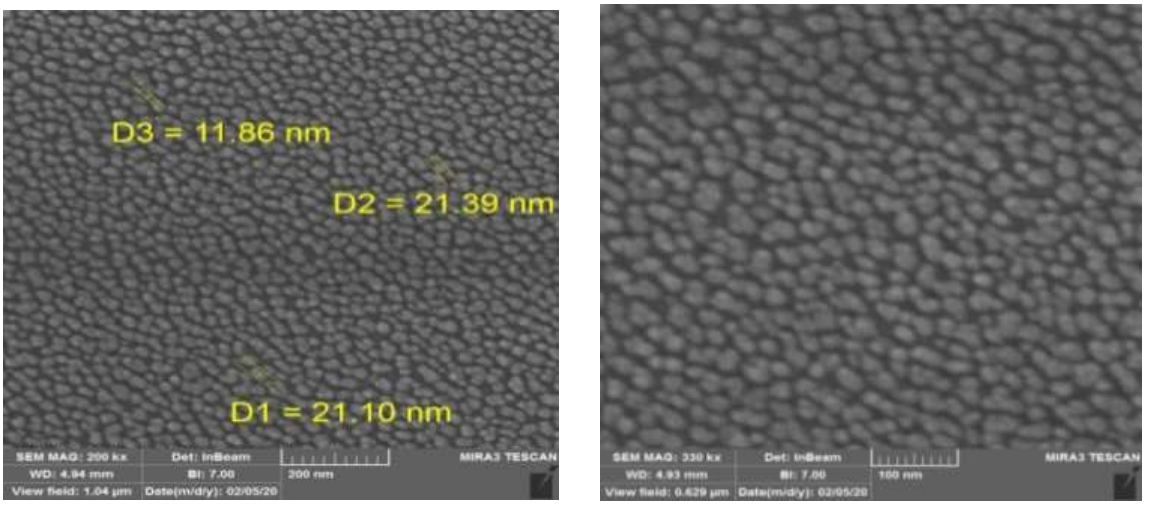

Fig. (7): SEM image of biosynthesized silver nanoparticles (a) The particle size at different average diameter D1, D2 and D3. (b) SEM shows the spherical shape of particles.

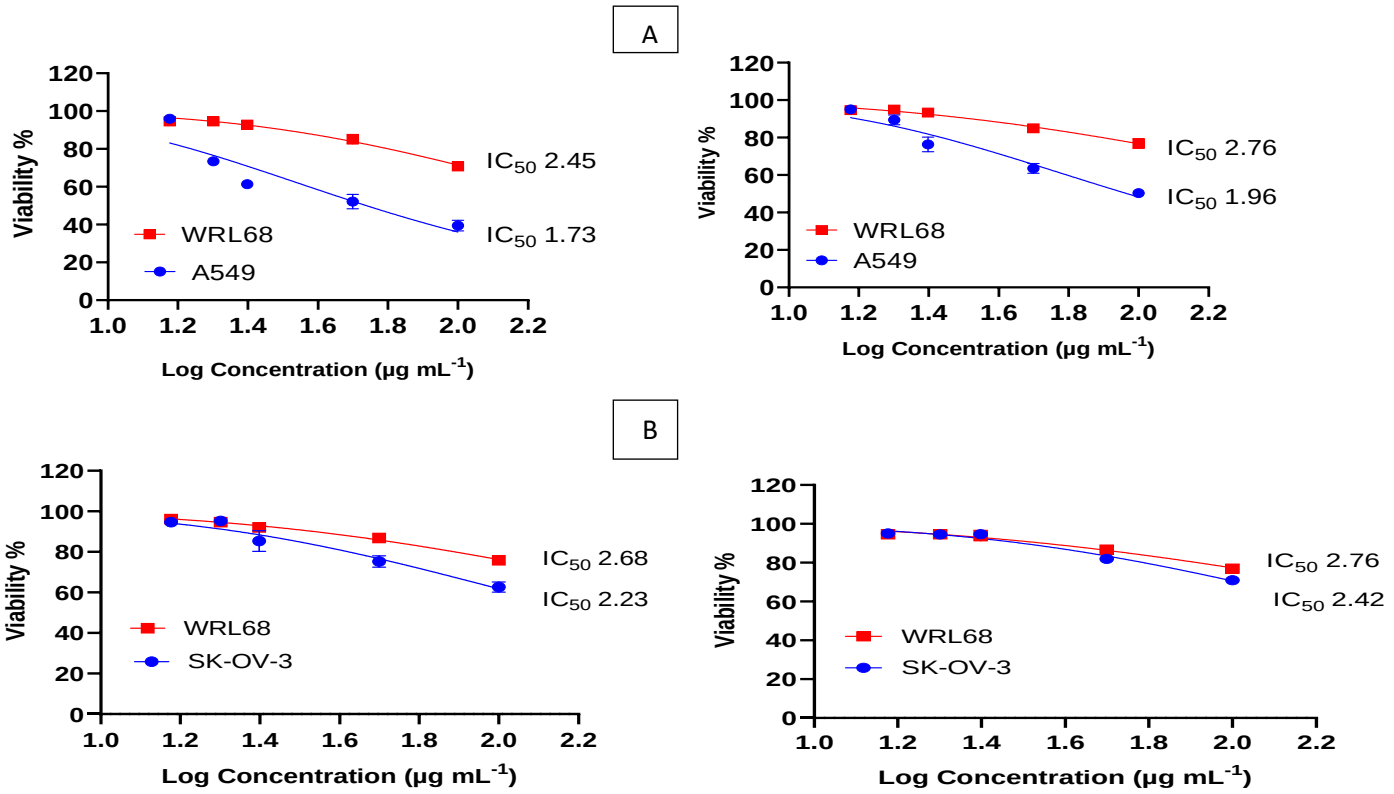

Fig. (8): The viability of (A) A549 cells for AgNPs and *D. viscosa* extract (B) SK-OV-3 cells for AgNPs and *D. viscosa* extract comparing with normal cell WRL68.

Anti-tumor Activity

The 3-(4,5-dimethylthiazol-2-yl)-2,5-diphenyl-2H-tetrazolium bromide (MTT) assay was used to assess cytotoxic potency of synthesized AgNPs. MTT assay in this study tested the viability of two cell line (human cancer cell lines A549 (lung cancer) and SK-OV-3 (ovarian cancer) and compared with normal cells line WRL68. After 24 hours of treatment with various concentration of leaves

extracts and AgNPs (15, 20, 25, 50 and 100 $\mu g.ml^{-1}$). The cytotoxicity results showed reduction in cell viability in a dose-dependent manner (Fig. 8). The A549 cell proliferation was significantly repressed by AgNPs with an IC_{50} value of 1.73 $\mu g.ml^{-1}$, as demonstrated in (Table 2). The SK-OV-3 cell lines, on the other hand, exhibited reproduction inhibition by AgNPs with an IC_{50} value of 2.23 $\mu g\ mL^{-1}$ compared to the viability of normal cell line WRL68 (human liver cells) exposed to the same concentration of AgNPs (Table 2). MTT cell viability using *D. viscosa* plant extract was also determined against the same cell lines used in the previous assay. A549 cell line incubated with the *D. viscosa* plant extract exhibited viability impairment with an IC_{50} value of 1.96 $\mu g.ml^{-1}$. The SKOV3 cell line showed similar viability reduction with an IC_{50} value of 2.42 $\mu g.ml^{-1}$. The MTT results for both AgNPs and the *D. viscosa* plant extract indicate a potential anti-cancer activity associated with higher concentrations against A549 in a dose-dependent manner and both AgNPs and extract are more sensitive towards A549 cell lines than SK-OV-3.

Table (2): Inhibition concentrations (IC_{50}) for cytotoxic activity of *D. viscosa* extract and synthesized silver nanoparticles on human lung cancer (A549) and ovarian cancer (SKOV3) compared with normal cells.

Log Concentration (µg/mL)	Cell line	%Cell viability	%Cell inhibition	IC_{50} (µg /mL)	Normal cell	%Cell viability	%Cell inhibition	IC_{50} (µg /mL)
2.000	A549 (Nano)	39.429	60.571	1.73*	WRL68	70.795	29.205	2.45
1.699		52.122	47.878			85.185	14.815	
1.398		61.381	38.619			92.824	7.176	
1.301		73.457	26.543			94.560	5.440	
1.176		95.949	4.051			94.560	5.440	
2.000	A549 (Ex.)	50.309	49.691	1.96	WRL68	76.890	23.11	2.76
1.699		63.503	36.497			84.915	15.085	
1.398		76.350	23.650			93.326	6.674	
1.301		89.429	10.571			94.946	5.054	
1.176		95.023	4.977			94.637	5.363	
2.000	SKOV3 (Nano)	62.654	37.346	2.23	WRL68	75.810	24.19	2.68
1.699		75.270	24.730			86.806	13.194	
1.398		85.340	14.660			92.052	7.948	
1.301		95.216	4.784			94.637	5.363	
1.176		94.637	5.363			96.181	3.819	
2.000	SKOV3 (Ex.)	70.988	29.012	2.42	WRL68	76.968	23.032	2.76
1.699		81.983	18.017			86.728	13.272	
1.398		94.637	5.363			93.981	6.019	
1.301		94.560	5.440			94.599	5.401	
1.176		95.062	4.938			94.599	5.401	

Ex.: *D. viscosa* extract

Nano: Synthesized silver nanoparticles

*Significant difference (p- Value <0.001)

Discussion

In recent years, for Ag nanoparticles biosynthesis, several plant extracts have been used. Plant extracts contents play as effective reducing as well as capping agent without addition of any further chemical components (Krishnaraj *et al.*, 2014). The GC-mass analysis displayed the existence of phytochemical components in *D. viscosa* leaf extract (Table1). Most of these compounds have biological activity (Saranya & Divyabharathi, 2019). Identifying the biological active compounds of *D. viscosa* leaf extract facilitates the therapeutic application of this plant for various diseases. The primary compound was 9, 12-octadecadienoic-acid, which is the main fatty acid in the extract. This fatty acid is characterized for several applications in the biomedical field. (anti-arthritic, anti-inflammatory, and antioxidant properties and used in the commercial preparation of oleates and lotions and as pharmaceutical solvent) (Srinivasan & Priya, 2019).

The first proof for synthesis of Ag nanoparticles is color change from yellow to the dark brown which indicates reducing of Ag^+ to Ag. The formation of AgNPs depends on how long the reducing agents are exposed to metal ions. Therefore, when the incubation period of silver with the reducing agent increase, the synthesis of AgNPs would increase more (Rocchetti *et al*., 2017). Characterization of Ag nanoparticles is essential to assure the synthesis of AgNPs and know whether the preparation is suitable for a specific application. Ultraviolet-vis Spectroscopy exhibited a clear peak at a wavelength of 463 nm. Formation and stability of AgNPs by *D. viscosa* extract in an aqueous medium is due to the effect of surface plasmon resonance (SPR) of an electron in the reaction mixture (Revathi & Dhanaraj, 2019). Dependent on the quantum size effects, these (SPR) bands undergo red-shift or blue-shift (Balashanmugam and Kalaichelvan, 2014). The solution's color shifts gradually from pale yellow to brown, indicate to formation of AgNPs. The broad absorption band is perfect for silver nanoparticles due to excitation of SPR where the peak shows that the particles are spherical with an extensive range of size distribution (Raza *et al*., 2016).

To determine the interaction of NPs and biomolecules, FT-IR analysis was performed to identify the active groups of these molecules. These materials are responsible for the capping, performance, and stabilization of metal nanoparticles (Daniel *et al.*, 2013). FTIR measurement of *D. viscosa* extract and AgNPs showed several peaks that represent several functional groups such as hydroxyl group (-OH) 3394.83 cm^{-1} and carboxyl group (-C=O) 1610.61 cm^{-1} related to extracting and shifted to 3331.18 cm^{-1} and 1620.26 cm^{-1} respectively. These groups act as reducing agents and stabilizer which and prevent particles agglomeration. The bending and stretching sensations display that biomolecules such as alcoholic groups, polyphenols, carboxylic acid, and proteins are responsible in the reduction Ag^+ and stabilizing of the AgNPs (Zafar *et al*., 2018). Supposedly the soluble compounds in plant extract in water such as flavonoids, terpenoids are the adsorbed molecules on the surface of NPs. The band at 759.98 cm^{-1} shows aromatic groups (-C=H). In plant extract, the existence of this bands re indicate to reduction

of flavonoids, proteins and sugars (Muniyappan and Nagarajan, 2014). The FTIR analysis showed that flavonoids and phytochemical compounds of the plant extracts act as reducing and stabilizing agent through the biosynthesis of NPs (Bethu *et al*., 2018).

XRD results illustrate the crystalline structure and purity of the produced NPs. The Brag reflection at 38.1874º, 46.2491º, 54.8851º, 57.5409º, and 76.8313º at 2θ values, confirmed the crystalize structure of silver nanoparticles. Bragg's law is a principle for the action of X-ray diffraction (Waseda *et al.*, 2011). Generally, X-ray diffraction is based on X-ray elastic wide-angle scattering. Values of these angles were comparing with those 2θ of AgNPs standard sample. When X-ray passing through a crystal it produces a diffraction pattern, that diffraction provides the information about the atomic arrangement within the crystals. (Srinivasan *et al.*, 2014).

AFM analysis determined the average mean size of the produced AgNPs is 60.22 nm. Previous studies have shown that the synthesis of AgNPs from commercially available plant extracts such as (*Centella asiatica, Solanum tricobatum Citrus sinensis,* and *Syzygium cumini)* have different unorganized forms with the particles size 53, 41, 52, and 42 nm respectively (Flaih and Al-Saadi, 2020). In the another study, the average size of AgNPs synthesized from the *Peltophorum pterocarpum* plant extract was in the same average size of the particles in the current study (Annamalai *et al*., 2018).

SEM image analysis of surface morphology of AgNPs showed a precise spherical shape without any agglomeration (Vivek *et al*., 2012).

Based on the results obtained from MTT assay, the cytotoxic potency of AgNPs mediated by a plant extract of *D. viscosa* was tested against A549 and SKOV3 cell lines and compared to normal cell line WRL68. There was moderate cytotoxic for AgNPs and extract of *D. viscosa* against A549 with an IC_{50} value of 1.73 and 1.96 µg mL^{-1} respectively, but there was less or no activity for AgNPs and *D. viscosa* against SKOV3 with an IC_{50} value of 2.23 and 2.42 µg ml^{-1} respectively. Besides, AgNPs and extract of *D. viscosa* shows weak cytotoxic on normal cell line WRL68 and IC_{50} range between 2.45-2.76 µg ml^{-1}. These results indicate does not get IC_{50}% in SKOV3 cell lines and normal cell lines WRL68 due to the inability of AgNPs and extract of *D. viscosa* to inhibit 50% from cell viability The finding of this study is in a good agreement of previous studies where they showed anti-cancer activity of produced AgNPs in *Cleome viscosa* fruit extract against A549 (lung) and PA1 (ovaries) cell lines at 28 and 30 µg/mL, respectively. The anticancer effect of AgNPs was more obvious on lung cancer cells than ovarian cancer cells (Lakshmanan *et al*., 2018). (Sriranjani *et al*., 2016) showed cytotoxic effect of biosynthesis silver nanoparticles against human colorectal adenocarcinoma (HT29) and Ehrlich ascites cell carcinoma (EAC). As well as, biosynthesized Ag nanoparticles in *Chaenomeles sinensis* and *Cibotium barometz* demonstrated anti-cancer efficacy against (MCF-7) cells (Oh *et al*., 2018; Wang *et al*., 2017). The use of plants as a medium for the synthesis of AgNPs showed a toxic effect on cancer cell lines A549 to see the cell-specific activity of AgNPs more than SK-OV-3 and normal cells. (Gurunathan *et al*., 2015). This study's results were consistent with the

previous studies that showed exposure to Ag nanoparticles could lead to different changes in cell morphology and reduce cell vitality (Asharani *et al*., 2009; Mohammed *et al*., 2018). The mechanism of the anticancer activity of silver nanoparticles involve, the entry of AgNPs into the cell lead to its damage by forming stable S-Ag bond with a thiol group of enzyme in cell membrane and its deactivation; or breaking Hydrogen bonds between Nitrogen bases of DNA and thereby denaturing it (Patil & Kumbhar, 2017). In general, it was found that the AgNPs synthesized in the green methods have broad activity against cancer cells in dose-dependent manner with no or little toxicity to normal cells.

Conclusions

Silver NPs showed significant role in many clinical applications. Cytotoxic agents against human cancer cell lines are one of the most important applications of synthesized AgNPs. In this study, one of the most important observations is that the synthesized silver nanoparticles (AgNPs) can inhibit cancer cell growth in a dose-dependent manner. Interestingly, green synthesized AgNPs showed more effect on lung cancer than ovarian cancer cells, with the lowest concentration of IC_{50} at 1.73 and 2.23 $\mu g.ml^{-1}$ respectively. Anticancer application of AgNPs open a new avenue in both fields to curing cancer and treating infectious diseases.

Acknowledgment

The authors are grateful to the staff of Department of Chemistry, College of Science, University of Kerbala, Iraq for their assistance during the procession of work, and also special thanks to Miss Hanin for her assistant in sample analysis by FTIR.

Conflicts of interest

The authors declare that they have no conflict of interests.

ORCID: Narjis H. Al-Saadi:

https://orcid.org/0000-0002-1396-9377

References

Alasmari, A. (2020). Phytomedicinal potential characterization of medical plants (*Rumex nervosus* and *Dodonaea viscose*). *Journal of Biochemical Technology*, *11*, 113-121. https://jbiochemtech.com/en/article/phytomedicinal potential-characterization-of-medical-plants rumex-nervosus-and-dodonaea-viscose

Abdelghany, T., Al-Rajhi, A. M., Al Abboud, M. A., Alawlaqi, M., Magdah, A. G., Helmy, E. A., & Mabrouk, A. S. (2018). Recent advances in green synthesis of silver nanoparticles and their applications: About future directions. A review. *BioNanoScience*, *8*, 5-16. https:// doi:10.1007/s12668-017-0413-3

Annamalai P, Balashanmugam P, Kalaichelvan P. (2018). Biogenic synthesis silver nanoparticles using *Peltophorum pterocarpum* leaf extracts and its antimicrobial efficacy against selective pathogens. *International Journal of Applied Pharmaceutics*. 10, 112-118. https://doi:10.22159/ijap.2018v10i6.28573

AshaRani, P. V., Low Kah Mun, G., Hande, M. P., *and* Valiyaveettil, S. (2009). Cytotoxicity and genotoxicity of silver nanoparticles in human cells. *ACS Nano*, *3*, 279-290. https://doi.org/10.1021/nn800596w

Balashanmugam, P., & Kalaichelvan, P. T. (2014). Biogenic synthesis of silver nanoparticles from *Dodonaea viscosa* Linn. and its effective antibacterial activity. *Scientific Transactions in Environment and Technovation*, *8*, 67-71. http://doi: 10.20894/STET.116.008.002.003

Barua, S., Konwarh, R., Bhattacharya, S. S., Das, P., Devi, K. S. P., Maiti, T. K., & Karak, N. (2013). Non-hazardous anticancerous and antibacterial

colloidal 'green'silver nanoparticles. *Colloids and Surfaces B: Biointerfaces, 105*, 37-42. http://doi:10.1016/j.colsurfb.2012.12.015

Bedlovičová, Z., & Salayová, A. (2017). *Green-Synthesized Silver Nanoparticles and Their Potential for Antibacterial Applications.* 73-94. In Kırmusaoğlu, S., (Editor). *Bacterial Pathogenesis and Antibacterial Control.* 154pp. http://dx.doi.org/10.5772/intechopen.72138

Bethu, M. S., Netala, V. R., Domdi, L., Tartte, V., & Janapala, V. R. (2018). Potential anticancer activity of biogenic silver nanoparticles using leaf extract of *Rhynchosia suaveolens*: an insight into the mechanism. *Artificial Cells, Nanomedicine, and Biotechnology*, *46*, 104-114. https://doi.org/10.1080/21691401.2017.1414824

Birla, S. S., Gaikwad, S. C., Gade, A. K., and Rai, M. K. (2013). Rapid synthesis of silver nanoparticles from *Fusarium oxysporum* by optimizing physicocultural conditions. *The Scientific World Journal, 013*. https://doi.org/10.1155/2013/796018

Daniel, S. K., Vinothini, G., Subramanian, N., Nehru, K., & Sivakumar, M. (2013). Biosynthesis of Cu, ZVI, and Ag nanoparticles using *Dodonaea viscosa* extract for antibacterial activity against human pathogens. *Journal of Nanoparticle Research*, *15*, 1319.https:// doi: 10.1007/s11051-012-1319-1

Flaih, L. S., & Al-Saadi, N. H. (2020). Characterization and clinical application of silver nanoparticles synthesized from *Cassia Obtusifoli*a leaves extract. *Plant Archives*, *20*, 1082-1088. https://www.researchgate.net/publication/342851985

Gasque, K. C. D. S., Al-Ahj, L. P., Oliveira, R. C., & Magalhães, A. C. (2014). Cell density and solvent are critical parameters affecting formazan evaluation in MTT assay. *Brazilian Archives of Biology and Technology*, *57*, 381-385. http://dx.doi.org/10.1590/S1516-89132014005000007

Gomaa, E. Z. (2017). Antimicrobial, antioxidant and antitumor activities of silver nanoparticles synthesized by *Allium cepa* extract: a green approach. *Journal of Genetic Engineering and Biotechnology*, *15*, 49-57. http://dx.doi.org/10.1016/j.jgeb.2016.12.002

Gopinath, K., Kumaraguru, S., Bhakyaraj, K., Mohan, S., Venkatesh, K. S., Esakkirajan, M., & Benelli, G. (2016). Green synthesis of silver, gold, and silver/gold bimetallic nanoparticles using the *Gloriosa superba* leaf extract and their antibacterial and antibiofilm activities. *Microbial Pathogenesis*, *101*, 1-11. https://doi: 10.1016/j.micpath.2016.10.011

Gurunathan, S., Jeong, J.-K., Han, J. W., Zhang, X.-F., Park, J. H., & Kim, J.-H. (2015). Multidimensional effects of biologically synthesized silver nanoparticles in *Helicobacter pylori*, *Helicobacter felis*, and human lung (L132) and lung carcinoma A549 cells. *Nanoscale research letters*, *10*, 1-17. https:// doi:10.1186/s11671-015-0747-0

Hamadi, S. S. (2017). Chemical study of Dodonaea viscosa planting in Iraq. *International Journal of Advances in Chemical Engineering, & Biological Sciences*, *4*, 121-125. https://doi.org/10.15242/IJACEBS.C0317025

Krishnaraj, C., Muthukumaran, P., Ramachandran, R., Balakumaran, M., & Kalaichelvan, P. (2014). *Acalypha indica* Linn: biogenic synthesis of silver and gold nanoparticles and their cytotoxic effects against MDA-MB-231, human breast cancer cells. *Biotechnology Reports*, *4*, 42-49. https://doi:10.1016/j.btre.2014.08.002

Lakshmanan, G., Sathiyaseelan, A., Kalaichelvan, P., & Murugesan, K. (2018). Plant-mediated synthesis of silver nanoparticles using fruit extract of *Cleome viscosa* L.: Assessment of their antibacterial and anticancer activity. *Karbala International Journal of Modern Science*, *4*, 61-68. https://doi.org/10.1016/j.kijoms.2017.10.007

Mahyoub, J. A. (2019). Biological effects of synthesized silver nanoparticles using *Dodonaea viscosa* leaf extract against *Aedes aegypti* (Diptera: Culicidae) *Journal of Entomology and Zoology Studies*, *7*, 827-832. https://www.entomoljournal.com/archives/2019/vol7issue1/PartM/7-1-97-583.pdf

Mohammed, A. E., Al-Qahtani, A., Al-Mutairi, A., Al-Shamri, B., & Aabed, K. (2018). Antibacterial and cytotoxic potential of biosynthesized silver nanoparticles by some plant extracts.

Nanomaterials, 8, 382. https://doi.org/10.3390/nano8060382

Moosa, A. A., Ridha, A. M., & Al-Kaser, M. (2015). Process parameters for green synthesis of silver nanoparticles using leaves extract of *Aloe vera* plant. *International Journal of Multidisciplinary and Current Research, 3*, 966-975. http://ijmcr.com

Muniyappan, N., & Nagarajan, N. (2014). Green synthesis of silver nanoparticles with Dalbergia spinosa leaves and their applications in biological and catalytic activities. *Process Biochemistry, 49*, 1054-1061. https://doi.org/10.1016/j.procbio.2014.03.015

Netala, V. R., Kotakadi, V. S., Domdi, L., Gaddam, S. A., Bobbu, P., Venkata, S. K., &. Tartte, V. (2016). Biogenic silver nanoparticles: efficient and effective antifungal agents. *Applied Nanoscience, 6*, 475-484. https:// doi:10.1007/s13204-015-0463-

Oh, K. H., Soshnikova, V., Markus, J., Kim, Y. J., Lee, S. C., Singh, P., & Shim, Y. J. (2018). Biosynthesized gold and silver nanoparticles by aqueous fruit extract of *Chaenomeles sinensis* and screening of their biomedical activities. *Artificial Cells, Nanomedicine, and Biotechnology, 46*, 599-606.https://doi.org/10.1080/21691401.2017.1332636

Otunola, G. A., & Afolayan, A. J. (2018). In vitro antibacterial, antioxidant and toxicity profile of silver nanoparticles green-synthesized and characterized from aqueous extract of a spice blend formulation. *Biotechnology & Biotechnological Equipment, 32*, 724-733. https://doi.org/10.1080/13102818.2018.1448301

Patil Shriniwas, P. (2017). Antioxidant, antibacterial and cytotoxic potential of silver nanoparticles synthesized using terpenes rich extract of Lantana camara L. leaves. *Biochemistry and Biophysics Reports, 10*, 76. https://doi: 10.1016/j.bbrep.2017.03.002

Raza, M. A., Kanwal, Z., Rauf, A., Sabri, A. N., Riaz, S., & Naseem, S. (2016). Size-and shape-dependent antibacterial studies of silver nanoparticles synthesized by wet chemical routes. *Nanomaterials, 6*, 74. https://doi.org/10.3390/nano6040074

Revathi, N., and Dhanaraj, T. (2019). Synthesis of silver nanoparticles from Dodonaea angustifolia leaf extract and evaluation of its anti-inflammatory activity. *Pramana Research Journal, 9*, 1118-1126. https://www.pramanaresearch.org/gallery/prj-p1138.pdf

Rocchetti, G., Lucini, L., Chiodelli, G., Giuberti, G., Montesano, D., Masoero, F., & Trevisan, M. (2017). Impact of boiling on free and bound phenolic profile and antioxidant activity of commercial gluten-free pasta. *Food Research International, 100*, 69-77. https://doi.org/10.1016/j.foodres.2017.08.031

Rojas, A., Cruz, S., Ponce-Monter, H., & Mata, R. (1996). Smooth muscle relaxing compounds from Dodonaea viscosa5. *Planta medica, 62*, 154-159. hptts://doi:10.1055/s-2006-957840

Saranya, K., & Divyabharathi, U. (2019). Gas Chromatography and mass Spectroscopic Analysis of Phytocompounds in *Dodonaea viscosa* leaves extract. *Pramana Research Journal*, 9, 26-35. https://www.pramanaresearch.org/gallery/prj-p1302.pdf

Singh, H., Du, J., & Yi, T.-H. (2017). Green and rapid synthesis of silver nanoparticles using *Borago officinalis* leaf extract: anticancer and antibacterial activities. *Artificial cells, Nanomedicine, and Biotechnology, 45*, 1310-1316. https://doi.org/10.1080/21691401.2016.1228663

Srinivasan, P., Sudhakar, S., Sengottaiyan, A., Subramani, P., Sudhakar, C., & Thiyagarajan, K. M. P. (2014). Green synthesis of silver nanoparticles using Cassia auriculata flower extract and its antibacterial activity. *International Journal of Advanced Science and Engineering, 1*, 42-46. https://www.mahendrapublications.com

Srinivasan, S., & Priya, V. (2019). Phytochemical screening and GC-MS analysis of *Cyperus dubius*, Rottb. (Cyperaceae). *Journal of Medicinal Plants, 7*, 89-98. https://www.plantsjournal.com/archives/?year=2019&vol=7&issue=2&part=B&ArticleId=961

Sriranjani, R., Srinithya, B., Vellingiri, V., Brindha, P., Anthony, S. P., Sivasubramanian, A., & Muthuraman, M. S. (2016). Silver nanoparticle synthesis using *Clerodendrum phlomidis* leaf extract

and preliminary investigation of its antioxidant and anticancer activities. *Journal of Molecular Liquids, 220*, 926-930. https://doi:10.1016/j.molliq.2016.05.042

Vivek, R., Thangam, R., Muthuchelian, K., Gunasekaran, P., Kaveri, K., & Kannan, S. (2012). Green biosynthesis of silver nanoparticles from Annona squamosa leaf extract and its *in vitro* cytotoxic effect on MCF-7 cells. *Process Biochemistry, 47*, 2405-2410. https://doi:10.1016/j.procbio.2012.09.025

Wang, D., Markus, J., Wang, C., Kim, Y.-J., Mathiyalagan, R., Aceituno, V. C., & Yang, D. C. (2017). Green synthesis of gold and silver nanoparticles using aqueous extract of *Cibotium barometz* root. *Artificial cells, Nanomedicine, and Biotechnology, 45*, 1548-1555. https://doi.org/10.1080/21691401.2016.1260580

Waseda, Y., Matsubara, E., & Shinoda, K. (2011). *X-ray diffraction crystallography: introduction, examples and solved problems*: Springer Science & Business Media. 310pp. https://doi:10.1007/978-3-642-16635-8

Yadi, M., Mostafavi, E., Saleh, B., Davaran, S., Aliyeva, I., Khalilov, R., & Panahi, Y. (2018). Current developments in green synthesis of metallic nanoparticles using plant extracts: A review. *Artificial cells. Nanomedicine, and Biotechnology, 46*, S336-S343. https://doi.org/10.1080/21691401.2018.1492931

Zafar, S., Ashraf, A., Ashraf, M. Y., Asad, F., Perveen, S., Zafar, M. A., & Shahzadi, A. (2018). Preparation of Eco-friendly Antibacterial Silver Nanoparticles from Leaf Extract of *Ficus benjamina*. *Biomedical Journal, 9, 7260-7264*. https://doi:10.26717/BJSTR.2018.09.001829

Zhang, X. F., Liu, Z. G., Shen, W., & Gurunathan, S. (2016). Silver nanoparticles: synthesis, characterization, properties, applications, and therapeutic approaches. *International Journal of Molecular Sciences, 17*, 1534 https://doi.org/10.3390/ijms17091534

النشاط المضاد للاورام لجسيمات الفضة النانوية المصنعة من مستخلص أوراق *Dodonaea viscosa*

زينب فيصل حبيب الموسوي[1] و نرجس هادي منصور السعدي[2]

قسم الكيمياء، كلية العلوم، جامعة كربلاء، العراق

المستخلص: التخليق الحيوي لجزيئات الفضة النانوية من المستخلصات النباتية تعتبر احد طرق الكيمياء الخضراء حيث تتميز هذه الطريقة بالسهولة و الكلفة المنخفضة بالأضافة الى انها تكون سريعة وصديقة للبيئة. ان جزيئات الفضة النانوية لها دور مهم خاصة في طب النانو. تعد جزيئات الفضة النانوية وسيلة ميسورة التكلفة للسيطرة على نمو الورم و اختيار استراتيجية في مكافحة السرطانات . الانظمة التقليدية لعلاج السرطان هي العلاج الاشعاعي و الكيميائي.مع ذلك فان هذه الانواع من علاج السرطان تعمل لبعض الانواع الفرعية للسرطان و قد تظهر اثارا جانبية للجرعات العالية. في هذا البحث تم تصنيع جزيئات الفضة النانوية من مستخلص اوراق الددونيا. تم التاكد من تكوين هذه الجسيمات خلال تغير اللون و الطيف الضوئي المرئي بالاشعة فوق البنفسجية عند النطاق 463,و طيف الاشعة تحت الحمراء الذي يحدد المجاميع الوظيفية الفعالة التي لها القدرة على اختزال ايون الفضة. استخدمت حيود الاشعة السينية لتحديد التركيب البلوري لجسيمات الفضة النانوية كما هو موضح في القمم عند قيم,38.1874, 46.2491, 57.54092, و º 76.8313. التحليل المجهري للقوة الذرية بين حجم و خصائص السطح للجسيمات النانوية المصنعة حيويا, و جسيمات الفضة النانوية بينت بان الجسيمات تمتلك متوسط حجم 60.22 نانومتر. صورة الفحص الجهري الالكتروني بينت الشكل الكروي لجسيمات الفضة النانوية كما وان لها متوسط قطر مختلف ,D1(21.10) D2 (21.39), D3 (11.86). ان هذه الجسيمات اظهرت فعالية ضد الاورام لخلايا الرئة السرطانية وخلايا المبايض السرطانية عند IC_{50} 1.73 و 2.23 مايكروكرام لكل مل على التوالي. اظهرت النتائج ان جزيئات الفضة النانوية يمكن ان تستخدم كعلاج بديل للسرطان بشكل مباشر و انتقائي على سرطان الرئة عند تراكيز2.000, 1.699, 1.398 و 1.301 مايكرو غرام/ مليلتر بشكل مباشر وانتقائي لخليتين مختلفتين.

الكلمات المفتاحية:جزيئات الفضة النانوية, الددونيا فسكوزا, مضاد للاورام, التخليق الحيوي.